Journal of Sound and Vibration (1997) **202**(2), 145–160

NORMAL MULTI-MODES OF NON-LINEAR EULER BEAMS

A. Y. T. Leung

*Department of Engineering, University of Manchester M*13 9*PL, England*

AND

T. Ge

Department of Mechanical Engineeering, University of Michigan, MI 48128, *U.S.A.*

(*Received* 5 *September* 1995, *and in final form* 9 *October* 1996)

For a strongly non-linear multi-degree-of-freedom system, in general, one cannot consider one mode at a time as in linear modal analysis. In the absence of external excitation, the natural vibration often involves more than one mode at a time resulting in quasi-periodic or multi-periodic (toroidal) vibration. The normal multi-mode in free vibration have been formulated by means of the action-angle transformation and the resulting ordinary differential equations embedded in partial differential equations. Final multi-periodic solutions have been obtained by extending the newly developed Toeplitz Jacobian matrix method with multi-periodic fast Fourier transforms.

1. INTRODUCTION

The authors are interested in the non-linear normal multi-modes of coupled systems of two or more degrees of freedom. Since the principle of superposition is no longer applicable to non-linear systems, one cannot decouple the non-linear systems directly. Recent research on non-linear normal modes is limited to the development of the most representative and the simplest description of the existing non-linear multi-degrees-of-freedom (MDOF) systems such that further explicit approximation can be made to the equations of motion. The classical theory of non-linear normal modes appeared as early as the 1960's. Rosenberg [1] classified non-linear normal modes into two types: similar mode and non-similar mode. The motion corresponding to a similar mode takes place along a straight line passing through the equilibrium position in the n dimensional configuration space whereas the motion corresponding to a non-similar mode occurs on a curved line passing through the equilibrium position in that space. This definition was implemented in much subsequent research to construct the non-linear normal modes of conservative two-degrees-of-freedom systems such as those of Rand [2], Vakakis [3], Vakakis and Rand [4, 5], and Rand *et al*. [6]. More recently, the concept of invariant manifold has been introduced for the illustration of non-linear normal modes. Shaw and Pierre [7, 8] developed an elegant approach for illustrating the non-linear normal modes of conservative as well as non-conservative oscillators. They argued that, for either linear or non-linear systems, a normal mode solution is one in which the system behaves like a single-degree-of-freedom (SDOF) system and can be represented by a two-dimensional manifold. For linear systems, these manifolds are the linear eigenspaces, whereas for non-linear systems, these manifolds are curved surfaces. It is evident that, for weakly non-linear systems these manifolds are tangent to the planar eigenspaces at the equilibrium point. Shaw and Pierre [9] applied their approach to construct the non-linear normal modes of a linear Euler–Bernoulli beam on a non-linear elastic foundation. Only the

0022–460X/97/170145 + 16 $25.00/0/sv960830

mono-mode was considered in their system. Nayfeh and Nayfeh [10] also studied non-linear modes of a one dimensional continuous system using the invariant manifold and multiple scale perturbation method. They supposed that the contribution of the other modes is of the smaller order quantities compared with those of the homogeneous solutions of leading mode.

On the other hand, the problem of geometrically non-linear or large amplitude free vibrations of beams has been investigated by many researchers, using approximate analytical methods and numerical methods such as finite elements. Woinowsky–Krieger [11], Srinavasan [12] and Ray and Bert [13] studied the large amplitude free vibrations of uniform beams using elliptic integral, perturbation and Ritz–Galerkin methods respectively. Finite element solutions to the problem were presented by Rao *et al*. [14], C. Mei [15, 16], Bennouna and White [17], Benamar *et al*. [18] and Singh *et al*. [19]. More recently Leung and Mao [20] applied the symplectic integration scheme in conjunction with an accurate beam finite element to solve the same problem. They found that non-linear mode interaction is inevitable for the free vibration of beams exhibiting quasi-periodic motions rather than periodic motions. Nevertheless, since many of the aforementioned methods for non-linear modes are limited in their applications to periodic vibration, in general, they cannot provide an accurate description of the behavior of beams with almost periodicity. Lau *et al*. [21] presented an almost periodic solution of a free vibrating beam using the incremental harmonic-balance (IHB) method with multiple time scales. However, since they treated the modal frequency as an unknown constant in a numerical way, they were unable to investigate the non-linear normal multi-modes.

In this paper, a multiple-periodic expression for normal modes along with the concept of the invariant manifold is established. Starting from the recognition that the free vibration of a beam is in fact a multiple-periodic motion, an invertible co-ordinate transformation by action-angles is introduced to configure the normal modes with different periodic units. Therefore, one can handle the modal interactions between the incommensurable natural frequencies in general. The accurate modal magnitudes are exploited by the multi-periodic Toeplitz Jacobian Matrix/Fast Fourier Transform (TJM/FFT) algorithm developed previously [22] together with the invariant embedding technique. The authors have shown in [23, 24] that the TJM method could obtain solutions much more efficiently than the IHB method. Embedding the ordinary differential equations in time variable onto partial differential equations (PDE) will capture the special dynamic features efficiently. A useful formula which leads to the explicit expression of linearized modal frequency is given. A numerical comparison with the existing results of multiple-mode free vibration is performed.

2. INVARIANT NORMAL MODE MANIFOLD

As illustrated by Carr [25], the computation of an n dimensional invariant manifold can be reduced to the computation of an invariant curve for an associated Poincaré map. The embedded PDE approach provides a natural connection between these two solutions. An obvious advantage is that the implicit dependent variable of time t can be eliminated from the original unknown objects and the resultant new system has one less dimension. The whole operation is in the core of invariant embedding techniques. Consider a particular set of first order non-linear differential equations depicted by a group of generalized co-ordinates

$$\dot{x}_i = \omega_i y_i, \qquad \dot{y}_i = -\omega_i x_i + f_i(x_1, x_2, \ldots, x_q; y_1, y_2, \ldots, y_q)/\omega_i, \quad i \in \mathbf{N}[1, q], \tag{1}$$

where (x_i, y_i) are state variables of the ith linear modal co-ordinate; ω_i the linear natural frequency of the ith linear normal mode; f_i denotes the non-linear part of the equations and q is the total number of degrees of freedom. The equations of motion can be separated into q independent linear modal equations when neglecting the non-linear actions. To simplify the problem with non-linear coupling, a functional dependent form is introduced in which all displacements and velocities are constrained to a finite dimensional manifold described by polar co-ordinates

$$x_i = r_i \sin \theta_k, \qquad y_i = r_i \cos \theta_k \quad k \in \mathbf{N}[1, p], \tag{2}$$

where θ_k stands for the action-angle variable in a certain polar co-ordinate. The resultant orbit equations for all the (r_i, θ_i) pairs can then describe either closed orbits or periodic functions of θ_i. Consequently, an invariant normal mode manifold T is denoted in p space by

$$T^p = \{\Theta = (\theta_1, \theta_2, \ldots, \theta_p) \colon \theta_i \in \mathbf{R} (\mathrm{mod}\, 2\pi)\}. \tag{3}$$

in which the function mod(2π) gives real module 2π. The governing equations (1) become

$$\mathrm{d}\Theta/\mathrm{d}t = \Omega + \mathbf{f}(\Theta, \mathbf{r}), \qquad \mathrm{d}\mathbf{r}/\mathrm{d}t = \mathbf{g}(\Theta, \mathbf{r}), \tag{4a, b}$$

where $(\Theta, \mathbf{r}) \in T^p \times \mathbf{R}^q$ and functions f: $T^p \times \mathbf{R}^q \to \mathbf{R}^p$, g: $T^p \times \mathbf{R}^q \to \mathbf{R}^p$ are assumed to be smooth; and $\Omega = \mathrm{diag}[\omega_i]$. The derivative of the action angle $\mathrm{d}\theta_i/\mathrm{d}t$ gives the frequency associated with the periodic motion of θ_i. The use of an action-angle variable thus provides a powerful technique for obtaining the frequency of periodic motion without finding a complete solution to the motion of the system. Similar to that illustrated in [8], any motion which satisfies equations (4) and (2) is defined to be a non-linear normal mode

$$M = \{(\Theta, \mathbf{r}(\Theta)) \colon \Theta \in T^p\} \subset T^p \times \mathbf{R}^q. \tag{5}$$

One further takes the time derivative of constraint equations (2) and uses the chain rule for differentiation to obtain the following PDE

$$\mathbf{w} = \sum_{j=1}^{p} [\omega_j + f_j(\Theta, \mathbf{r}(\Theta))] \frac{\partial \mathbf{r}}{\partial \theta_j}(\Theta) - \mathbf{g}(\Theta, \mathbf{r}(\Theta)) \equiv 0, \qquad \Theta \in T^p, \tag{6}$$

where $\mathbf{w}$ is used as a note of zero invariant expression and the periodic boundary conditions of radii r_i are implemented with

$$r_i(\theta_1, \ldots, \theta_{k-1}, 0, \theta_{k+1}, \ldots, \theta_p) = r_i(\theta_1, \ldots, \theta_{k-1}, 2\pi, \theta_{k+1}, \ldots, \theta_p),$$
$$i \in \mathbf{N}[1, q], \quad k \in \mathbf{N}[1, p]. \tag{7}$$

It should be emphasized that this characterization of the motion does not mean that each r_i and θ_i will necessarily be periodic functions of time, i.e., that they repeat their values at fixed time intervals. Even when each of the separated (r_i, θ_i) pairs is indeed periodic in this sense, the overall system motion need not be periodic. Thus, in a MDOF system the frequencies of motion along the different modal co-ordinates may all be different. The complete motion of the system may not always be periodic. If the frequencies are not rational fractions of each other, the system will not travel along a closed curve in space but will demonstrate an open "Lissajous" figure. Such motion will be described as multi-periodic. It is an advantage of the action-angle variables that they lead to an evaluation of all the frequencies involved in multi-periodic motion without requiring a complete solution of the motion.

3. MULTI-PERIODIC TJM/FFT ALGORITHM

Compared to the original ODEs (1), an obvious advantage of the PDE expression (6) lies in the explicit periodicity of the independent parameters θ_k. The solutions of the non-linear partial differential equations (6) are difficult to express analytically, thus apparently precluding spectral analysis where a closed form representation of the manifold is to be sought. The TJM/FFT method for spectral analysis can be used here so that samples of the coefficients are taken over one complete period and are fed to a computer algorithm to find the invariant manifold.

The pair of multi-periodic Fourier transform for vectors $\{\mathbf{r}\}$ and $\{\mathbf{w}\}$ can be defined in the same way as that in the mono-periodic case [26, 27],

i) Inverse Fourier transform

$$\begin{bmatrix} r_i(\theta_1, \theta_2, \ldots, \theta_p) \\ w_i(\theta_1, \theta_2, \ldots, \theta_p) \end{bmatrix} = \sum_{k_1=-N_1}^{N_1} \sum_{k_2=-N_2}^{N_2} \cdots \sum_{k_p=-N_p}^{N_p} \begin{bmatrix} R_i(k_1, k_2, \ldots, k_p) \\ W_i(k_1, k_2, \ldots, k_p) \end{bmatrix} \cdot \mathrm{e}^{\mathrm{i}(k_1\theta_1 + k_2\theta_2 + \cdots + k_p\theta_p)} + \text{h.o.t.} \tag{8}$$

ii) Fourier transform

$$\begin{bmatrix} R_i(k_1, k_2, \ldots, k_p) \\ W_i(k_1, k_2, \ldots, k_p) \end{bmatrix} = \frac{1}{(2\pi)^p} \int_0^{2\pi} \int_0^{2\pi} \cdots \int_0^{2\pi} \begin{bmatrix} r_i(\theta_1, \theta_2, \ldots, \theta_p) \\ w_i(\theta_1, \theta_2, \ldots, \theta_p) \end{bmatrix} \cdot \mathrm{e}^{-\mathrm{i}(k_1\theta_1 + k_2\theta_2 + \cdots + k_p\theta_p)} \, \mathrm{d}\theta_1 \, \mathrm{d}\theta_2 \cdots \mathrm{d}\theta_p, \tag{9}$$

where k_i represents the wave number, R_i and W_i are spectral counterparts of functions r_i and w_i respectively, and h.o.t. stands for "higher order terms". The above mentioned process was named the Galerkin procedure [28]. The resulting set of simultaneous equations in Eq. (6) is non-linear and therefore, the Newton-Raphson algorithm is pursued to seek the unknowns in a predictor-corrector manner e.g., $\{\mathbf{R}\} = \{\mathbf{R}\}_0 + \{\Delta\mathbf{R}\}$, in which the subscription zero represents the nearby solution vector of the equations, $\{\Delta\mathbf{R}\}$ is the unknown incremental vector given by:

$$[\mathbf{J}]\{\Delta\mathbf{R}\} = \{\mathbf{Z}\}, \tag{10}$$

where $[\mathbf{J}]$ is the analytical Jacobian matrix

$$J_{i,j} = (\partial W_i / \partial R_j), \qquad i, j \in \mathbf{N}[-N, N] \tag{11}$$

and $\{\mathbf{Z}\}$ is the right hand residual vector used in the iteration.

If one denotes

$$\mathbf{Dr} = \partial\mathbf{r}/\partial\Theta = [\partial r_i / \partial\theta_k], \tag{12}$$

the variations can be introduced in order to represent the perturbations of $\mathbf{r}$, $\mathbf{Dr}$ at a given position Θ,

$$w_i(\mathbf{r}_0 + \Delta\mathbf{r}, \mathbf{Dr}_0 + \Delta\mathbf{Dr}, \Theta) = w_i(\mathbf{r}_0, \mathbf{Dr}_0, \Theta) + \sum_{k=1}^{p} \left.\frac{\partial w_i}{\partial (D_k r_i)}\right|_0 \Delta D_k r_i + \sum_{j=1}^{q} \left.\frac{\partial w_i}{\partial r_j}\right|_0 \Delta r_j + \text{h.o.t.} = 0, \tag{13}$$

where the parametrized functions α_k and $\beta_{i,j}$ are defined respectively by

$$\alpha_k = \left.\frac{\partial w_i}{\partial (D_k r_i)}\right|_0 = f_k^0, \qquad \beta_{i,j} = \left.\frac{\partial w_i}{\partial r_j}\right|_0 = \left[\sum_{k=1}^{p} \frac{\partial f_k}{\partial r_j} \cdot \frac{\partial r_i}{\partial \theta_k} - \frac{\partial g_i}{\partial r_j}\right]^0; \tag{14}$$

and the perturbed function ξ_i is selected according to its use as predictor or corrector

$$\xi_i = \begin{cases} \left.\dfrac{\partial w_i}{\partial r_k}\right|_0 \Delta r_k & \text{predictor} \\ w_i(\mathbf{r}_0, \mathbf{D}\mathbf{r}_0, \Theta) & \text{corrector} \end{cases}. \tag{15}$$

Here, Δr_k refers to the prescribed control increment. Sampling each phase plane with $[M_1, M_2, \ldots, M_p]$ interval-equivalent discrete points respectively and substituting the backward Fourier transform (8) into equation (13), one has

$$\begin{aligned} w_i(s_1, s_2, \ldots, s_p) = \sum_{k_1=-N_1}^{N_1} \sum_{k_2=-N}^{N_2} \cdots \sum_{k_p=-N_p}^{N_p} \Bigg[\sum_{j=1}^{q} \beta_{i,j}(s_1, s_2, \ldots, s_p) \\ + \mathrm{i} \sum_{j=1}^{p} k_j \alpha_j(s_1, s_2, \ldots, s_p) \Bigg] \Delta R_i(k_1, k_2, \ldots, k_p) \cdot \mathrm{e}^{\mathrm{i}\sum_{j=1}^{p} 2\pi s_j k_j / M_j} \\ + \xi_i(s_1, s_2, \ldots, s_p) + \text{h.o.t.} = 0. \end{aligned} \tag{16}$$

In order to avoid aliasing distortions in the above sampling process, the requisite number of retaining points are given by $M_k \geqslant 2N_k + 1$ [26, 27].

After applying the inverse discrete Fourier transform and interchanging the order of summations, one obtains

$$\begin{aligned} W_i(l_1, l_2, \ldots, l_p) = \sum_{k_1=-N_1}^{N_1} \sum_{k_2=-N}^{N_2} \sum_{k_p=-N_p}^{N_p} \Bigg[\sum_{j=1}^{q} B_{i,j}(l_1 - k_1, l_2 - k_2, \ldots, l_p - k_p) \\ + \mathrm{i} \sum_{j=1}^{p} k_j A_j(l_1 - k_1, l_2 - k_2, \ldots, l_p - k_p) \Bigg] \\ \cdot \Delta R_i(k_1, k_2, \ldots, k_p) + Z_i(l_1, l_2, \ldots, l_p) = 0, \end{aligned} \tag{17}$$

where A_{i-j} and B_{i-j} are the components of the Toeplitz matrices [**A**] and [**B**] which can be evaluated directly by applying the inverse fast Fourier transform algorithm to the parametrized functions α and β respectively,

$$\begin{aligned} A_j(\tau_1, \tau_2, \ldots, \tau_p) = \frac{1}{M_1 M_2, \ldots, M_p} \sum_{s_1=0}^{M_1-1} \sum_{s_2=0}^{M_2-1} \cdots \sum_{s_p=0}^{M_p-1} \alpha_j(s_1, s_2, \ldots, s_p) \\ \cdot \mathrm{e}^{-\mathrm{i}\sum_{j=1}^{p} 2\pi s_j \tau_j / M_j}, \end{aligned}$$

$$B_{i,j}(\tau_1, \tau_2, \ldots, \tau_p) = \frac{1}{M_1 M_2, \ldots, M_p} \sum_{s_1=0}^{M_1-1} \sum_{s_2=0}^{M_2-1} \cdots \sum_{s_p=0}^{M_p-1} \beta_{i,j}(s_1, s_2, \ldots, s_p)$$

$$\cdot \mathrm{e}^{-\mathrm{i} \sum_{j=1}^{p} 2\pi s_j \tau_j / M_j}, \tag{18}$$

where τ_j denotes the index of the convolution sequences used by the Toeplitz matrices,

$$\tau_j = \mathrm{mod}((M_j + l_j - k_j)/M_j), \qquad l_m, k_m \in \mathbf{N}[-N_m, N_m], \quad m = 1, p. \tag{19}$$

Therefore, the Jacobian matrix used in the Newton–Raphson iteration is given by

$$\partial W_i(l_1, l_2, \ldots, l_p)/\partial R_i(k_1, k_2, \ldots, k_p) = \sum_{j=1}^{q} B_{i,j}(l_1 - k_1, l_2 - k_2, \ldots, l_p - k_p)$$

$$+ \mathrm{i} \sum_{j=1}^{p} k_j A_j(l_1 - k_1, l_2 - k_2, \ldots, l_p - k_p). \tag{20}$$

The right side vector is determined directly by the inverse fast Fourier transform of the perturbed function ξ,

$$Z_i(l_1, l_2, \ldots, l_p) = \frac{1}{M_1 M_2, \ldots, M_p} \sum_{s_1=0}^{M_1-1} \sum_{s_2=0}^{M_2-1} \cdots \sum_{s_p=0}^{M_p-1} \xi_i(s_1, s_2, \ldots, s_p) \cdot \mathbf{e}^{-\mathrm{i} \sum_{j=1}^{p} 2\pi s_j l_j / M_j}. \tag{21}$$

4. APPLICATION

The governing equation describing the transverse vibration of an elastic beam with large slenderness ratio and immovable ends is known to be [16]

$$\rho A \frac{\partial^2 y}{\partial t^2} + EI \frac{\partial^4 y}{\partial x^4} - \left[\frac{EA}{2L} \int_0^L \left(\frac{\partial y}{\partial x} \right)^2 \mathrm{d}x \right] \frac{\partial^2 y}{\partial x^2} = 0, \tag{22}$$

where ρ is the beam density; E is Young's modulus; A, L and I are the cross-section area, the length of the beam and the moment of inertia respectively; y denotes the transverse deflection of the beam and x represents its axial axis; t is the time. The non-linearity in equation (22) is caused by the axial membrane force due to the end constraints. However, the curvatures of the beam during deflection are assumed to be small and both shear deformations and longitudinal inertia have been neglected in this model. The solution of equation (22) can be expressed as a series in terms of the linear free oscillation modes $\phi_m(x)$,

$$y(x, t)/r = \sum_{m=1}^{\infty} u_m(t) \phi_m(x), \tag{23}$$

where u_m represents the magnitude of the mth mode of the beam; $r = \sqrt{I/A}$ is the radius of gyration. Substituting equation (23) into equation (22), multiplying by ϕ_m and integrating over the beam length, one has

$$\ddot{u}_m + \omega_m^2 u_m + \sum_{n,p,q=1}^{\infty} \Gamma_{mnpq} u_n u_p u_q = 0, \tag{24}$$

where

$$\Gamma_{mnpq} = \frac{1}{2} \int_0^1 \frac{\partial \phi_m}{\partial \chi} \frac{\partial \phi_n}{\partial \chi} \, \mathrm{d}\chi \int_0^1 \frac{\partial \phi_p}{\partial \chi} \frac{\partial \phi_q}{\partial \chi} \, \mathrm{d}\chi, \quad \chi = \frac{x}{L}, \tag{25}$$

and

$$\Gamma_{mnpq} = \Gamma_{nmpq} = \Gamma_{mnqp} = \Gamma_{pqmn}. \tag{26}$$

If the first two modes of the elastic beam are of interest, then one has

$$y(x, t)/r = u_1(t)\phi_1(x) + u_2(t)\phi_2(x). \tag{27}$$

Consequently, the following set of 2-DOF non-linear ordinary differential equations can be obtained

$$\begin{aligned} &\ddot{u}_1 + \omega_1^2 u_1 + a_{130} u_1^3 + a_{12} u_1^2 u_2 + a_{112} u_1 u_2^2 + a_{103} u_2^3 = 0, \\ &\ddot{u}_2 + \omega_2^2 u_2 + a_{230} u_1^3 + a_{221} u_1^2 u_2 + a_{212} u_1 u_2^2 + a_{203} u_2^3 = 0, \end{aligned} \tag{28}$$

where ω_k is the kth ratio of natural frequency, $\omega_1 = 1$, $\omega_2 = (\lambda_2/\lambda_1)^2$; λ_1, λ_2 are the first two roots of the frequency equation; the coefficients $a_{k,i,j}$ $(k = 1, 2; i + j = 3)$ are constants evaluated by Γ_{mnpq} $(m, n, p, q = 1, 2)$,

$$a_{k30} = \frac{1}{\lambda_1^4} \Gamma_{k111}, \; a_{k21} = \frac{1}{\lambda_1^4} (\Gamma_{k112} + \Gamma_{k121} + \Gamma_{k211}), \qquad a_{k12} = \frac{1}{\lambda_1^4} (\Gamma_{k112} + \Gamma_{k212} + \Gamma_{k221}),$$

$$a_{k03} = (1/\lambda_1^4)\Gamma_{k222}; \quad k = 1, 2.$$

Let $x_i = u_1$, $y_1 = \dot{u}_1/\omega_1$, $x_2 = u_2$, $y_2 = \dot{u}_2/\omega_2$, then

$$\begin{aligned} &\dot{x}_1 = \omega_1 y_1, \qquad \dot{y}_1 = -\omega_1 x_1 - (1/\omega_1)(a_{130} x_1^3 + a_{121} x_1^2 x_2 + a_{112} x_1 x_2^2 + a_{103} x_2^3), \\ &\dot{x}_2 = \omega_2 y_2, \qquad \dot{y}_2 = -\omega_2 x_2 - (1/\omega_2)(a_{230} x_1^3 + a_{221} x_1^2 x_2 + a_{212} x_1 x_2^2 + a_{203} x_2^3). \end{aligned} \tag{29}$$

Furthermore, if one transforms equation (29) into polar co-ordinates with $x_1 = r_1 \sin \varphi_1$, $y_1 = r_1 \cos \varphi_1$, $x_2 = r_2 \sin \varphi_2$, $y_2 = r_2 \cos \varphi_2$, one has

$$\begin{Bmatrix} \dot{\varphi}_k \\ \dot{r}_k \end{Bmatrix} = \begin{bmatrix} r_k \cos \varphi_k & \sin \varphi_k \\ -r_k \sin \varphi_k & \cos \varphi_k \end{bmatrix}^{-1} \begin{Bmatrix} \omega_k r_k \cos \varphi_k \\ -\omega_k r_k \sin \varphi_k - (1/\omega_k) f_k \end{Bmatrix}, \tag{30}$$

where f_k represents the non-linear parts in equations (29) and $k = 1, 2$. Equations (29) can be rewritten as

$$\begin{aligned} &\dot{\varphi}_1 = \omega_1 + (1/8\omega_1 r_1)\Psi_1(\varphi_1, r_1, \varphi_2, r_2), \qquad \dot{r}_1 = (1/8\omega_1)\mathscr{R}_1(\varphi_1, r_1, \varphi_2, r_2), \\ &\dot{\varphi}_2 = \omega_2 + (1/8\omega_2 r_2)\Psi_2(\varphi_1, r_1, \varphi_2, r_2), \qquad \dot{r}_2 = (1/8\omega_2)\mathscr{R}_2(\varphi_1, r_1, \varphi_2, r_2), \end{aligned} \tag{31}$$

where

$$\begin{aligned}
\Psi_1(\varphi_1, r_1, \varphi_2, r_2) &= 3a_{130}r_1^3 + 2a_{112}r_1r_2^2 - (4a_{130}r_1^3 + 2a_{112}r_1r_2^2)\cos 2\varphi_1 + a_{130}r_1^3\cos 4\varphi_1 \\
&\quad + 6(a_{121}r_1^2r_2 + a_{103}r_2^3)\sin\varphi_1\sin\varphi_2 - 2a_{103}r_2^3\sin\varphi_1\sin 3\varphi_2 \\
&\quad + 2a_{112}r_1r_2^2\cos 2\varphi_1\cos 2\varphi_2 - 2a_{121}r_1^2r_2\sin 3\varphi_1\sin\varphi_2 \\
&\quad - 2a_{112}r_1r_2^2\cos 2\varphi_2, \\
\mathscr{R}_1(\varphi_1, r_1, \varphi_2, r_2) &= -2(a_{130}r_1^3 + a_{112}r_1r_2^2)\sin 2\varphi_1 + a_{130}r_1^3\sin 4\varphi_1 \\
&\quad - 2(a_{121}r_1^2r_2 + 3a_{103}r_2^3)\cos\varphi_1\sin\varphi_2 + 2a_{103}r_2^3\cos\varphi_1\sin 3\varphi_2 \\
&\quad + 2a_{112}r_1r_2^2\sin 2\varphi_1\cos 2\varphi_2 + 2a_{121}r_1^2r_2\cos 3\varphi_1\sin\varphi_2, \\
\Psi_2(\varphi_1, r_1, \varphi_2, r_2) &= 2a_{221}r_1^2r_2 + 3a_{203}r_2^3 - (4a_{203}r_2^3 + 2a_{221}r_1^2r_2)\cos 2\varphi_2 + a_{203}r_2^3\cos 4\varphi_2 \\
&\quad + 6(a_{212}r_1r_2^2 + a_{203}r_1^3)\sin\varphi_1\sin\varphi_2 - 2a_{212}r_1r_2^2\sin\varphi_1\sin 3\varphi_2 \\
&\quad + 2a_{221}r_1^2r_2\cos 2\varphi_1\cos 2\varphi_2 - 2a_{230}r_1^3\sin 3\varphi_1\sin\varphi_2 \\
&\quad - 2a_{221}r_1^2r_2\cos 2\varphi_1, \\
\mathscr{R}_2(\varphi_1, r_1, \varphi_2, r_2) &= -2(a_{203}r_2^3 + a_{221}r_1^2\mathrm{r}_2)\sin 2\varphi_2 + a_{203}r_2^3\sin 4\varphi_2 \\
&\quad - 2(a_{212}r_1r_2^2 + 3a_{230}r_1^3)\sin\varphi_1\cos\varphi_2 + 2a_{212}r_1r_2^2\sin\varphi_1\cos 3\varphi_2 \\
&\quad + 2a_{221}r_1^2r_2\cos 2\varphi_1\sin 2\varphi_2 + 2a_{230}r_1^3\sin 3\varphi_1\sin\varphi_2.
\end{aligned}$$

Two separate partial differential equations can be obtained

$$\left(\omega_1 + \frac{1}{8\omega_1 r_1}\Psi_1\right)\frac{\partial r_1}{\partial\varphi_1} + \left(\omega_2 + \frac{1}{8\omega_2 r_2}\Psi_2\right)\frac{\partial r_1}{\partial\varphi_2} - \frac{1}{8\omega_2}\mathscr{R}_1 = 0,$$

$$\left(\omega_1 + \frac{1}{8\omega_1 r_1}\Psi_1\right)\frac{\partial r_2}{\partial\varphi_1} + \left(\omega_2 + \frac{1}{8\omega_2 r_2}\Psi_2\right)\frac{\partial r_2}{\partial\varphi_2} - \frac{1}{8\omega_2}\mathscr{R}_2 = 0. \tag{32}$$

Equations (32) represent an invariant normal multi-mode manifold in the parametric space φ_1, φ_2. The solutions of the modal magnitude r_1, r_2 can be obtained by means of the aforementioned multi-periodic TJM/FFT method. It should be noted that, as mentioned in the former section, the modal frequencies v_1, v_2 are actually given by the derivatives of action-angle $\dot{\varphi}_1$, $\dot{\varphi}_2$ which are also multi-periodic functions of φ_1, φ_2 as shown in Figure 1(a, b). However, to compare with those quantities obtained in the linear oscillation, one makes use of the multiple averaging technique to get the simple mean values,

$$\bar{v}_1 = \int_0^{2\pi}\int_0^{2\pi}\varphi_1\,\mathrm{d}\varphi_1\,\mathrm{d}\varphi_2 = \omega_1 + (1/8\omega_1)(3a_{130}r_1^2 + 2a_{112}r_2^2),$$

$$\bar{v}_2 = \int_0^{2\pi}\int_0^{2\pi}\varphi_2\,\mathrm{d}\varphi_1\,\mathrm{d}\varphi_2 = \omega_2 + (1/8\omega_2)(2a_{221}r_1^2 + 3a_{203}r_2^2) \tag{33}$$

Thus, the influence of modal interaction can be seen clearly. Table 1 gives the comparison of the present results with the existing one obtained by the IHB method. Figure 2(a) shows the variation of the first and second linearized mean frequencies against the mode magnitude R_{100} in which $\eta = R_{100}/R_{200}$ is specified to be 1, 2 and 10 respectively. It is interesting to note the first modal frequency boosts faster than the second one. As

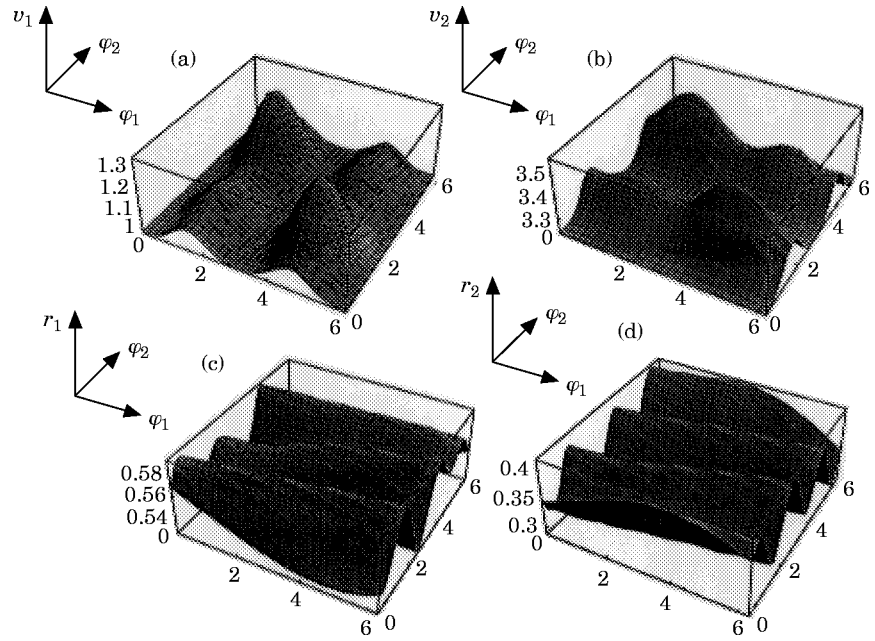

Figure 1. Surface diagram for mode frequencies and mode magnitudes.

a consequence, by the time $v_1 = v_2/3$ internal resonance takes place and the beam undergoes periodic motion. In other words, the system exhibits multi-periodic motion only if its natural frequencies are not rational fractions of each other. Otherwise the motion repeats after a sufficiently long time and would therefore be simply periodic. Moreover, it can be shown that the path of the multi-periodic motion is non-degenerated and fills a limit region of both the configuration spaces and the phase space (periodic surface). Whenever degeneracy is present the fundamental frequencies are no longer independent and the periodic motion of the system can be described by less than a full complement of system frequencies with the appearance of split bounds of the periodic trajectory. The ultimate boundary of R_{100} against the variation of $\eta = R_{100}/R_{200}$ is depicted in Figure 2(b). The curves are evaluated under two different degenerate conditions but the discrepancy between the two is minor.

(1) Suppose that internal resonance takes place at $v_1 = v_2/3$. Equation (33), yields

$$\max R_{100} = \sqrt{\frac{\omega_2}{3} - \omega_1 + \left(\frac{3a_{130} + 2a_{112}/\eta^2}{8\omega_1} - \frac{2a_{221} + 3a_{203}/\eta^2}{24\omega^2}\right)}. \tag{34}$$

TABLE 1

Mode magnitude values

	$R_{100} = 0{\cdot}3$		$R_{100} = 0{\cdot}5$		$R_{100} = 0{\cdot}7$	
$R_{100}/R_{200} = 2$	IHB	Present	IHB	Present	IHB	Present
$\bar{v}_1$	1·01559	1·01569	1·04271	1·04357	1·08485	1·0854
$\bar{v}_2$	3·25841	3·28992	3·28983	3·28992	3·33815	3·33745

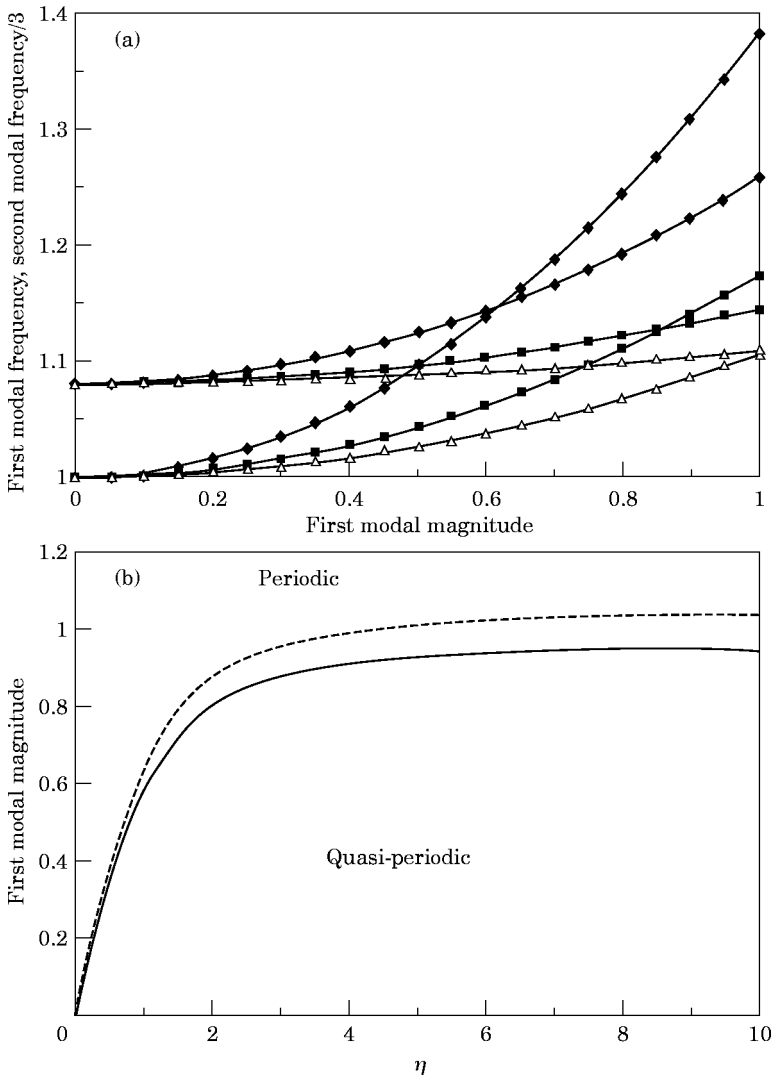

Figure 2. (a) The variation of the first two linearized mean frequencies against the mode magnitudes, η: —◆—, 1; —■—, 2; —△—, 10. (b) The ultimate boundary of R_{100} versus η.

(2) Suppose, more strictly, that internal resonance takes place when $\varphi_1 = \varphi_2/3$ and start from equation (29) with a new polar co-ordinate transformation: $x_1 = r_1 \sin \varphi_1$, $y_1 = r_1 \cos \varphi_1$, $x_2 = r_2 \sin 3\varphi_1$, $y_2 = r_2 \cos 3\varphi_1$, similar to that illustrated from equations (30) to (34), one then obtains a new expression

$$\max R_{100} = \sqrt{\frac{\omega_2}{3} - \omega_1 + \left(\frac{3a_{130} + 2a_{112}/\eta^2 - a_{121}/\eta}{8\omega_1} - \frac{2a_{221} + 3a_{203}/\eta^2 - a_{230}\eta}{24\omega^2} \right)}. \quad (35)$$

The inequality of (34) and (35) also reflects that the system is passing through a hyperbolic Hopf bifurcation point at which no cross-section point is found in the configuration space to connect those two different types of invariant manifolds. Trends of the curves shown in Figure 2(a, b) also clearly suggest that the degeneracy of the

invariant normal mode manifold corresponds closely to the increase of the modal magnitude. The aforementioned treatments are applicable to more general cases. By noting a symmetric relation exhibited from equation (29) to equation (33), further expressions for more modal frequencies can be derived by simple extrapolated relations, for example,

$$\bar{v}_1 = \int_0^{2\pi}\int_0^{2\pi}\int_0^{2\pi} \dot{\varphi}_1 \,\mathrm{d}\varphi_1 \,\mathrm{d}\varphi_2 \,\mathrm{d}\varphi_3 = \omega_1 + (1/8\omega_1)(3a_{1300}r_1^2 + 2a_{1120}r_2^2 + 2a_{1102}r_2^2)$$

$$\bar{v}_2 = \int_0^{2\pi}\int_0^{2\pi}\int_0^{2\pi} \dot{\varphi}_2 \,\mathrm{d}\varphi_1 \,\mathrm{d}\varphi_2 \,\mathrm{d}\varphi_3 = \omega_2 + (1/8\omega_2)(2a_{2210}r_1^2 + 2a_{2012}r_3^2 + 3a_{2030}r_2^2)$$

$$\bar{v}_3 = \int_0^{2\pi}\int_0^{2\pi}\int_0^{2\pi} \dot{\varphi}_3 \,\mathrm{d}\varphi_1 \,\mathrm{d}\varphi_2 \,\mathrm{d}\varphi_3 = \omega_3 + (1/8\omega_3)(2a_{2201}r_1^2 + 2a_{2021}r_2^2 + 3a_{2003}r_3^2) \text{ etc.} \tag{36}$$

where $a_{m,i,j,k}$, $i + j + k = 3$, $m = 1, 2, 3$, are coefficients given by the Galerkin method. The complete set of double periodic solutions is in the form of

$$\begin{bmatrix} r_1(s_1, s_2) \\ r_2(s_1, s_2) \end{bmatrix} = \sum_{k_1=-N}^{N}\sum_{k_2=-N}^{N} \begin{bmatrix} R_1(k_1, k_2) \\ R_2(k_1, k_2) \end{bmatrix} \cdot \mathrm{e}^{\mathrm{i}[(2\pi s_1 k_1)/M_1 + (2\pi s_2 k_2)/M_2]}, \qquad s_1, s_2 \in \mathbf{N}[-N, N]. \tag{37}$$

However, in order to reduce the amount of computational work, further simplifications to the solution form are introduced,

$$\begin{bmatrix} r_1(s_1, s_2) \\ r_2(s_1, s_2) \end{bmatrix} = \sum_{\substack{k_1=0 \\ |k_1|+|k_2| \leqslant K_m}}^{N} \sum_{\substack{k_2=-N \\ k_1, k_2 = even}}^{N} \begin{bmatrix} R_1(k_1, k_2) \\ R_2(k_1, k_2) \end{bmatrix} \cdot \mathrm{e}^{\mathrm{i}2\pi(s_1 k_1 + s_2 k_2)/M} + \mathrm{cc}, \tag{38}$$

where cc stands for the complex conjugate of the proceeding terms. From previous experience, one knows that all periodic components

$$\upsilon_m = k_{1m}\varphi_1 + k_{2m}\varphi_2 \tag{39}$$

with

$$|k_{1m}| + |k_{2m}| \leqslant K_m \tag{40}$$

are likely to be eminent. Therefore, in this particular case one can choose $K_m = 12$, $N = K_m$, $m = 1, 2$ and consider only the waves whose numbers are included in equation (40). The periodic surfaces formed by the first and the second modal magnitudes are demonstrated in Figure 1(c, d) respectively. A representative double periodic solution by the TJM method is listed in Table 2. The overall quasi-periodic motion of equation (27) at $x = 0{\cdot}25L$ is presented in Figure 3(a). In practical computations, a control increment factor should be prescribed in the ways by physical rather than purely numerical consideration. For example, to reveal the multiply-periodic motion of free vibrating beam, one of the following strategies may be adopted. that is (1) two of the fundamental magnitudes R_{100}, R_{200} are fixed; (2) one fundamental magnitude R_{100} and the ratio of the two fundamental magnitudes R_{100}/R_{200} are fixed.

When one of these conditions is introduced, a curve on the solution surface is thus defined. The steps are similar to those described by Lau *et al*. [21] but the efficiency of the procedure will be greatly improved by means of the multi-periodic TJM/FFT technique [22]. It was also pointed out in [22] that the invariant normal mode manifolds would be

more intuitively understood if they are presented in toroidal co-ordinates as shown in Figures 4(a)–(d). In addition, to see the accuracy of the linearized analysis by means of equation (33), the dynamic response of the Euler beam at $x = 0{\cdot}25L$ is approximated by

$$y(x, t)/r = \phi_1(0{\cdot}25L)R_{100} \sin \bar{\nu}_1 t + \phi_2(0{\cdot}25L)R_{200} \sin \bar{\nu}_2 t. \tag{41}$$

TABLE 2

Double periodic solution using the TJM method

k_1	k_2	$\lvert R_1(k_1, k_2)\rvert$	$\lvert R_2(k_1, k_2)\rvert$	R_1(Re)	R_1(Im)	R_2(Re)	R_2(Im)
0	0	0·5634	0·3589	0·5634E + 00	0·0000E + 00	0·3589E + 00	0·0000E + 00
0	2	0·0077	0·0002	−0·4933E − 02	−0·5885E − 02	−0·1416E − 03	−0·1680E − 03
0	4	0·0003	0·0001	0·5600E − 04	−0·3270E − 03	0·1642E − 04	−0·1075E − 03
0	6	0·0000	0·0000	−0·3820E − 04	0·2058E − 04	0·3872E − 04	−0·2081E − 04
0	8	0·0000	0·0000	−0·6424E − 05	−0·1155E − 05	0·8819E − 06	0·1621E − 05
0	10	0·0000	0·0000	−0·2361E − 05	0·1153E − 05	0·3086E − 07	0·4521E − 06
0	12	0·0000	0·0000	−0·1013E − 05	0·1021E − 05	−0·7420E − 06	0·1104E − 05
2	−10	0·0000	0·0000	−0·5719E − 05	−0·5328E − 05	0·4553E − 05	0·5449E − 05
2	−8	0·0001	0·0000	−0·4470E − 05	0·5703E − 04	−0·1834E − 05	−0·7134E − 05
2	−6	0·0002	0·0005	0·1809E − 03	−0·1480E − 03	0·3988E − 03	−0·2827E − 03
2	−4	0·0004	0·0002	0·3391E − 03	0·8764E − 04	0·2317E − 03	0·6219E − 04
2	−2	0·0011	0·0006	−0·4844E − 03	−0·1020E − 02	0·2678E − 03	0·5700E − 03
2	0	0·0000	0·0018	0·7586E − 05	−0·1882E − 04	−0·7318E − 03	0·1596E − 02
2	2	0·0005	0·0002	−0·5087E − 03	0·1417E − 03	−0·1994E − 03	0·5518E − 04
2	4	0·0000	0·0000	0·4068E − 04	0·2748E − 04	0·2222E − 04	0·1766E − 04
2	6	0·0000	0·0000	−0·5521E − 06	−0·1869E − 05	−0·3573E − 05	−0·1441E − 05
2	8	0·0000	0·0000	−0·1563E − 05	−0·1199E − 06	−0·1896E − 05	0·1099E − 05
2	10	0·0000	0·0000	0·8219E − 06	0·4408E − 06	−0·2736E − 05	0·9466E − 06
4	−8	0·0000	0·0000	−0·1028E − 04	−0·4813E − 05	0·1557E − 04	0·9407E − 05
4	−6	0·0000	0·0000	−0·2189E − 05	−0·7825E − 05	0·1795E − 06	0·1256E − 04
4	−4	0·0000	0·0000	0·1464E − 04	−0·1924E − 04	−0·1840E − 04	0·1925E − 04
4	−2	0·0000	0·0000	0·1633E − 05	0·4494E − 06	−0·2894E − 04	0·1055E − 05
4	0	0·0000	0·0002	−0·8494E − 06	−0·9142E − 06	0·1477E − 03	0·1705E − 03
4	2	0·0000	0·0000	0·1412E − 05	−0·9397E − 05	−0·2872E − 05	−0·6531E − 05
4	4	0·0000	0·0000	0·6339E − 06	−0·1239E − 05	−0·4231E − 05	0·2808E − 05
4	6	0·0000	0·0000	−0·1585E − 05	0·7045E − 07	−0·1440E − 05	0·1894E − 05
4	8	0·0000	0·0000	−0·4419E − 06	0·1092E − 05	−0·2368E − 05	0·1671E − 05
6	−6	0·0000	0·0000	0·3373E − 06	0·3367E − 06	−0·5936E − 05	−0·6396E − 06
6	−4	0·0000	0·0000	−0·5563E − 06	0·1527E − 05	−0·3790E − 05	−0·1968E − 05
6	−2	0·0000	0·0000	0·7223E − 06	−0·7167E − 06	−0·3650E − 05	0·6651E − 06
6	0	0·0000	0·0000	−0·7735E − 06	−0·5362E − 06	−0·8873E − 05	0·3593E − 05
6	2	0·0000	0·0000	−0·7753E − 06	0·2767E − 06	−0·2942E − 05	0·1481E − 05
6	4	0·0000	0·0000	−0·7455E − 06	0·5066E − 06	−0·2389E − 05	0·1023E − 05
6	6	0·0000	0·0000	−0·1643E − 06	0·6426E − 06	−0·1841E − 05	0·1322E − 05
8	−4	0·0000	0·0000	−0·1349E − 05	−0·1815E − 06	−0·1682E − 05	0·1258E − 05
8	−2	0·0000	0·0000	−0·6013E − 06	−0·4418E − 06	−0·1909E − 05	0·1656E − 05
8	0	0·0000	0·0000	−0·1224E − 05	−0·3291E − 06	−0·1202E − 05	0·2612E − 05
8	2	0·0000	0·0000	−0·9056E − 06	−0·1123E − 08	−0·7898E − 06	0·1989E − 05
8	4	0·0000	0·0000	−0·7024E − 06	0·1195E − 06	−0·9833E − 06	0·1976E − 05
10	−2	0·0000	0·0000	−0·3710E − 06	−0·7001E − 07	−0·2147E − 05	0·1086E − 05
10	0	0·0000	0·0000	−0·2138E − 07	−0·6332E − 07	−0·2662E − 05	0·1896E − 05
10	2	0·0000	0·0000	−0·6387E − 06	−0·5927E − 06	−0·1295E − 05	0·1681E − 05
12	0	0·0000	0·0000	−0·3149E − 06	−0·2639E − 06	−0·1095E − 05	0·1523E − 05

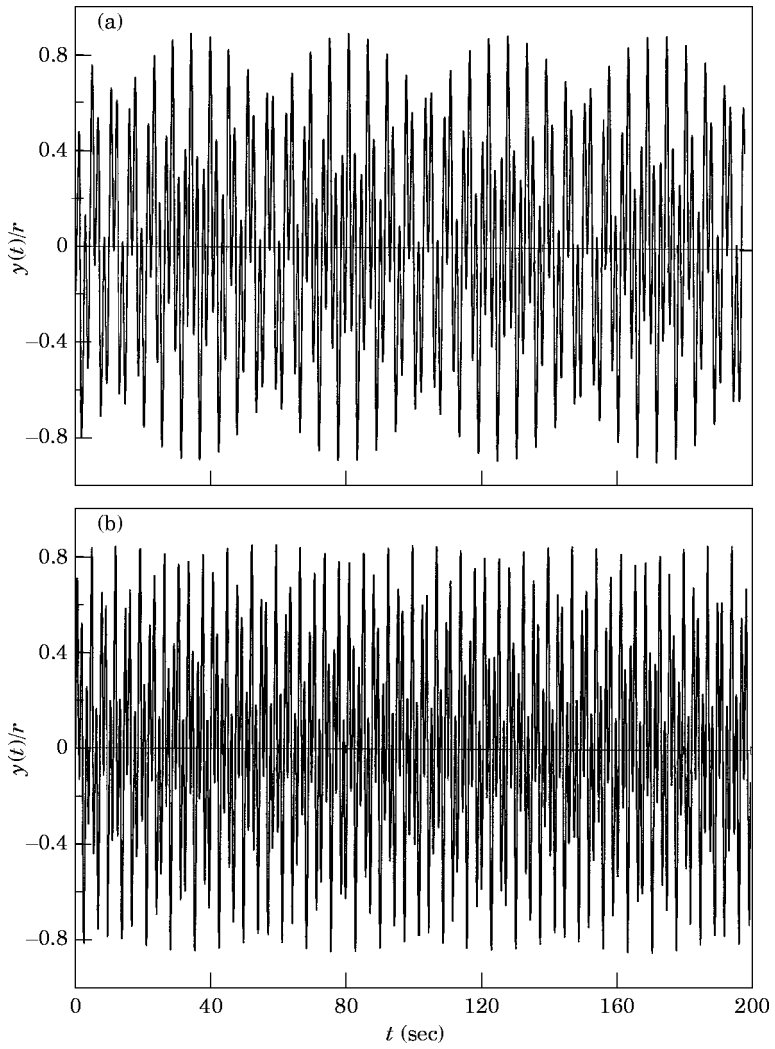

Figure 3. (a) The exact time history of equation (27). (b) The approximate time history of equation (27).

The time history of equation (41) is depicted in Figure 3(b). Compared to Figure 3(a), the outside wavelet has been shown to decay due to the negligence of the higher order harmonic terms in equation (31).

5. CONCLUSION

An alternative form for the non-linear normal modal manifold called the multi-mode is defined in this paper. The present definition is capable of treating the multi-mode interactive motion between the incommensurable natural frequencies of multiple DOF systems. The theory is exemplified by the multi-mode non-linear free vibration of an elastic beam. A multi-periodic TJM algorithm is also introduced to construct the invariant normal mode manifold, i.e., 2-torus etc. The other particular merit of the present treatment lies in the fact that the linearized non-linear natural frequency can be evaluated beforehand. However, the comparison with the incremental harmonic balance also shows a

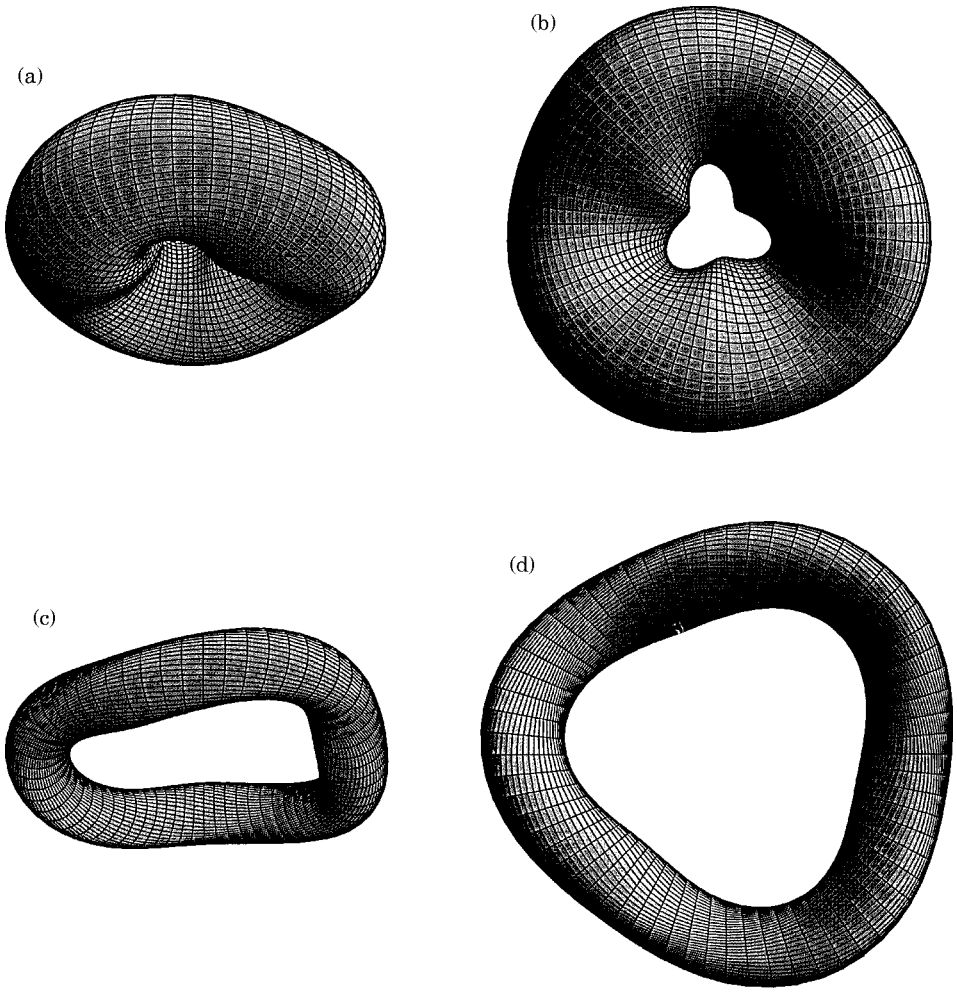

Figure 4. The invariant normal mode manifold in toroidal co-ordinates. (a) Viewpoint (1·4, −2·6, −1·8), $R_{100} = 0{\cdot}5634$, $R_{200} = 0{\cdot}3589$; (b) Viewpoint (0, 0, −1), $R_{100} = 0{\cdot}5634$, $R_{200} = 0{\cdot}3589$; (c) Viewpoint (1·4, −2·6, −1·8), $R_{100} = 0{\cdot}5415$, $R_{200} = 0{\cdot}1298$; (d) Viewpoint (0, 0, 1), $R_{100} = 0{\cdot}5415$, $R_{200} = 0{\cdot}1298$.

good agreement between the present linearization and existing results. The overall methodology can be considered as an attempt to generalize the theory of invariant normal mode manifold but the primary stability and bifurcation questions remain untouched as a challenging problem for future study. It is, perhaps, of some theoretical value to establish the complete theory of non-linear normal multi-mode and develop the explicit supposition method for a class of non-linear systems.

ACKNOWLEDGMENT

The research is supported by the Research Grant Council of Hong Kong.

REFERENCES

1. R. M. Rosenberg 1966 *Advances in Applied Mechanics* **9**, 155–242. On non-linear vibrations of systems with many degrees of freedom.

2. R. H. Rand 1974 *International Journal of Non-linear Mechanics* **9**, 363–368. A direct method for nonlinear normal modes.
3. A. Vakakis 1990 *Ph.D. Dissertation*, *California Institute of Technology*. Analysis and identification of linear and non-linear normal modes in vibrating system.
4. A. Vakakis and R. H. Rand 1992 *International Journal of Non-Linear Mechanics* **27**, 861–874. Normal modes and global dynamics of a two-degrees-of-freedom non-linear system-I. Low Energies.
5. A. Vakakis and R. H. Rand 1992 *International Journal of Non-Linear Mechanics* **27**, 875–888. Normal modes and global dynamics of a two-degrees-of-freedom non-linear system—II. High Energies.
6. R. H. Rand, D. H. Pak and A. Vakakis 1992 *Acta Mechanics* **3**, 129–145. Bifurcation of nonlinear normal mode in a class of two degree of freedom system.
7. S. W. Shaw and C. Pierre 1991 *Journal of Sound and Vibration* **150**, 170–173. Non-linear normal modes and invariant manifolds.
8. S. W. Shaw and C. Pierre 1993 *Journal of Sound and Vibration* **164**, 85–124. Normal modes for non-linear vibratory systems.
9. S. W. Shaw and C. Pierre 1992 *Nonlinear Vibrations ASME* 1992 DE-**50**/AMD-**144**, 1–5. On nonlinear normal modes.
10. A. H. Nayfeh and S. A. Nayfeh 1994 *ASME Journal of Vibration and Acoustics* **116**, 129–136. On Nonlinear modes of continuous systems.
11. S. Woinowsky-Krieger 1950 *Trans. ASME* **72**, 35–36. The effects of an axial force on the vibration of hinged bars.
12. A. V. Srinavasan 1965 *AIAA Journal* **3**, 1951–1953. Large amplitude free oscillations of beam and plates.
13. J. D. Ray and C. W. Bert 1969 *ASME Journal of Engineering for Industry* **91B**, 997–1004, Nonlinear vibrations of a beam with pinned ends.
14. G. V. Rao, K. K. Raju and I. S. Raju 1974 *Computers and Structures* **6**, 169–172. Finite element formulation for large amplitude free vibrations of slender beams and orthotropic circular plates.
15. C. Mei 1973 *AIAA Journal* **11**, 115–117. Finite element analysis of nonlinear vibrations of beam columns.
16. C. Mei 1973 *Computers and Structures* **3**, 163–174. Finite element displacement method for large amplitude free flexural vibrations.
17. M. M. K. Bennouna and R. G. White 1984 *Journal of Sound and Vibration* **96**, 309–331. The effects of large vibration amplitudes on the fundamental mode shape of clamped-clamped uniform beam.
18. R. Benamar, M. M. K. Bennouna and R. G. White 1991 *Journal of Sound and Vibration* **149**, 179–195. The effects of large vibration amplitudes on the mode shapes and natural frequencies of thin elastic structures. Part I: Simply supported and clamped-clamped beams.
19. G. Singh, A. K. Sharma and G. V. Rao 1990 *Journal of Sound and Vibration* **142**, 77–85. Large amplitude free vibrations of a beam—a discussion on various formulations and assumptions.
20. A. Y. T. Leung and S. G. Mao 1995 *Journal of Sound and Vibration* **183**, 475–491. A symplectic Galerkin method for non-linear vibration of beams and plates.
21. S. L. Lau, Y. K. Cheung and S. Y. Wu 1983 *American Society of Mechanical Engineers*, *Journal of Applied Mechanics* **51**, 871–876. Incremental harmonic balance method with multiple time scales for aperiodic vibration of nonlinear systems.
22. T. Ge and A. Y. T. Leung 1995 *Nonlinear Dynamics*. Construction of Invariant Torus of ODE Using PDE-TJM/FFT Approach (Submitted).
23. A. Y. T. Leung and T. Ge 1995 *American Society of Mechanical Engineers*, *Journal of Applied Mechanics* **117**. Toeplitz Jacobian method for nonlinear periodic oscillators.
24. T. Ge and A. Y. T. Leung 1995 *Shock and Vibration* **2**, 205–218. A Toeplitz Jacobian matrix/fast Fourier transformation method for steady-state analysis of discontinuous oscillators.
25. J. Carr 1981 *Applications of Center Manifold Theory*. New York: Springer-Verlag.
26. E. O. Brigham 1974 *The Fast Fourier Transformation*. New York: Prentice-Hall.
27. D. E. Newland 1975 *An Introduction to Random Vibration and Spectral Analysis*. London: Longman.
28. M. Urabe 1965 *Archives Rational Mechanics and Analysis* **20**, 120–152. Galerkin's procedure for nonlinear periodic systems.

APPENDIX

The development of natural non-linear modes of a beam is illustrated by clamped–hinged beams. The vibration behavior of such examples is of interest to many researchers [10, 20, 21] because the second linear natural frequency is nearly three times the fundamental frequency. Under such circumstances, internal resonance with periodic motions may occur whereas in the neighborhood of that state, the almost periodic motion widely exist due to the interaction of non-linear modes.

For clamped-hinged beam the boundary conditions are

$$w(0) = 0, \quad w''(0) = 0; \qquad w(L) = 0, \quad w''(L) = 0 \tag{A.1}$$

The linear mode shapes are given by

$$\phi_m(x) = \cosh \lambda_m x - \cos \lambda_m x - \frac{\cosh \lambda_m L - \cos \lambda_m L}{\sinh \lambda_m L - \sin \lambda_m L} (\sinh \lambda_m x - \sin \lambda_m x), \tag{A.2}$$

and the natural frequency λ_m are the roots of the frequency equation

$$\cosh \lambda L \sin \lambda L - \sinh \lambda L \cos \lambda L = 0, \tag{A.3}$$

and its first two roots are $\lambda_1 L = 3{\cdot}927$, $\lambda_2 L = 7{\cdot}069$ respectively. Substituting (A.2) into equation (27) yields the coefficients of equations (25) as $a_{130} = 0{\cdot}278769$, $a_{121} = -0{\cdot}311074$, $a_{112} = 1{\cdot}11585$, $a_{103} = -0{\cdot}386361$, $a_{230} = -0{\cdot}10369$, $a_{221} = 1{\cdot}11585$, $a_{212} = 1{\cdot}159083$, $a_{203} = 3{\cdot}87030$, $\omega_1 = 1$, $\omega_2 = 3{\cdot}2404$.